Integrated design optimization of the transmission system and vehicle control for electric vehicles

Preprints of the 20th World Congress
The International Federation of Automatic Control
Toulouse, France, July 9-14, 2017

Integrated design optimization of the transmission system and vehicle control for electric vehicles

T. Hofman* **and N.H.J. Janssen***

* *Eindhoven University of Technology, Den Dolech 2, 5600 MB, Eindhoven, The Netherlands (e-mail: t.hofman@tue.nl).*

Abstract: The focus is on the combined design optimization of the transmission design and control design for an electric vehicle. In literature, these design problems are treated separately, whereas combining both mathematically coupled design problems into an integrated problem improves optimality. A shiftable transmission, e.g., a continuously variable transmission (CVT), allowing a smooth and continuous transition between the powertrain operation points further optimizes the energy usage, yet also allows further the reduction of the electric machine (Nm/W) and transmission specifications (overall speed ratio) in comparison with an optimized fixed-gear transmission. Moreover, a CVT enables for autonomous driving electric vehicles to further increase the driving range without compromising the vehicle performance. The influence of the transmission type, losses and driving conditions (average speed) are investigated for an EV of which the travelled distance, velocity and speed ratio (for the CVT) are the controlled states.

Keywords: Hybrid and alternative drive vehicles; Adaptive and robust control of automotive systems; Nonlinear and optimal automotive control

1. INTRODUCTION

In literature, the research interests on the topic of co-design, or the integrated design of the plant artefact (hardware) and the control system (software) are increasing due to the increase of design complexity. In particular, for systems that have a strong mathematical coupling between the hardware and the software objectives and/or constraints as is the case with advanced hybrid and electric powertrains do require an integrated system design approach to achieve a global optimal design (Allison and Nazari, 2010).

1.1 Combined transmission and control design

Here, the focus is on the integrated design of the transmission system and control system for an electrical vehicle (EV). For the transmission system, two systems are selected, i.e., a fixed-gear (FGT) and a continuously variable transmission (CVT). Both transmission systems are optimized together with the electric machine (EM) size (maximum torque, power specification) and the travelled distance, vehicle velocity and speed ratio (for the CVT), as the controlled-state variables. In literature, some papers focus on the control design (Dib et al., 2014) or the transmission design individually, (Hofman and Dai, 2001), and, clearly, prove (battery) energy-saving potential by optimally controlling the vehicle velocity ('eco-driving') for a fixed powertrain design, or optimizing the transmission design (ratio coverage, or gear values) on a fixed (reference) drive cycle. This paper contributes on investigating mathematically the co-design problem, thereby, the problem is formulated as a nested (bi-level) optimization problem. In the outer layer (upper level), the transmission design is optimized and in the inner layer (bottom level), the control optimization is performed. The control design is for both transmission systems formulated as a two-point boundary value problem (TPBVP). For the CVT design case, an extra control input is defined with the gear speed ratio change. Pontryagin's Minimum Principle (PMP) (Pontryagin et al., 1962) is used for solving the problem, which will show that the CVT gear speed ratio as additional controlled state creates a 'bang-bang' type of control of the speed ratio due to singularities. A smoothing function is used to circumvent this problem, preventing that higher order derivatives of the Hamiltonian have to be considered in solving the problem. The paper organization is as follows, first, the control design problems (including the smoothing function) for both transmissions will be introduced in Section 2. This section starts with the modeling of the power train losses and the vehicle dynamics modeling for the EV. Accordingly, the co-design problem in Section 3; and, the influence of the transmission type, CVT losses and the driving conditions (average vehicle speed) on the optimal design (torque scale EM) and minimum energy consumption and control are investigated in Section 3.1, respectively. In the final Section 4, the conclusions and outlook will be summarized.

2. OPTIMAL CONTROL PROBLEM FOR AN ELECTRIC VEHICLE

Below the optimal control problem (OCP) for an EV with a fixed-gear (FGT) and a continuously variable transmission (CVT) will be introduced. The CVT is assumed to be of the pushbelt variator type (Vroemen, 2001). First, the power train loss model and the vehicle dynamics model will be briefly discussed.

2.1 Powertrain loss model

The focus is on energy consumption minimization, therefore, a powertrain model for the electric vehicle needs to be derived. Here, as in a similar fashion in (Dib et al., 2014), an energy usage function is formulated, but extended with additional loss terms to capture additional characteristics. Since, using the model from (Dib et al., 2014), would result in optimal speed ratio transmission design with an operating point with the angular velocity of the motor as large as possible and the torque of the motor as small as possible. Therefore, another simplified model is used here (Larminie and Lowry, 2003) that describes the machine input power, P_m as a function of the summation of the delivered motoring power, the friction, electric resistance, iron, windage power losses and a constant power loss term, respectively.

$$\begin{aligned} P_m(\tau(t),\omega(t)) = \tau(t)\cdot\omega(t) + b_1\ \tau(t)^2 \\ +b_2\ \omega(t) + b_3\ \omega(t)^3 + b_4 \end{aligned} \tag{1}$$

where ω and τ are the angular velocity and output torque of the motor in (rad/s) and (Nm) as a function of time t in (s). The parameters b_i can be used to fit the model onto the efficiency data. Without loss of generality, the efficiency data (incl. power electronics) of a 32-kW / 59-Nm (max. spd. 7000 rpm) permanent magnet motor controller (PMMC) combination from ADVISOR is used (Wipke et al., 2002). The efficiency of the PMMC can be calculated with,

$$\eta_m(t) = \min\left(\alpha(t), \alpha^{-1}(t)\right) = [0,1] \in \mathbb{R}^+ \tag{2}$$

with $\alpha(t) = (\tau(t)\cdot\omega(t))/P_m(t)$. The cost function, denoted as J, resulting from Eq. (1) is formed by its integral,

$$J = \int_0^T P_m\left(.\right)\ \mathrm{d}t \tag{3}$$

which is used to optimize the energy consumption of the EV (also regenerative braking is considered) starting at $t = 0$ s and ending at a fixed time $t = T$ s. Note depending on the transmission type, FGT or CVT, r depends on time t or not. The transmission ratio is defined as, respectively,

$$r(t) = \begin{cases} r_t & \text{for FGT,} \\ r_{CVT}(t)\cdot r_t & \text{for CVT} \end{cases} \tag{4}$$

where the CVT operation range is limited between an underdrive r_{max} and an overdrive value r_{min}. The sizing of the efficiency map is considered by using torque s_τ and speed scale parameters s_ω, whereby the efficiency and (maximum) power of the motor (and power electronics) is assumed to scale accordingly,

$$P_m = (\tau\cdot s_\tau)\cdot(\omega\cdot s_\omega) \tag{5}$$

For simplicity, the battery losses are left out of consideration.

2.2 Vehicle dynamics model

The vehicle load is determined by the rolling resistance, air drag losses and gradient resistance, respectively. Using Newton's second law of motion, the acceleration of the vehicle can be expressed as,

$$\dot{v}(t) = h_3(r(t))\cdot(\tau(t)-\tau_0) - h_2\cdot v(t)^2 - h_1(d(t)) - h_0 \tag{6}$$

with the parameters h_i defined as,

$$\begin{aligned} &h_0 = g\ c_r; \qquad h_1(d(t)) = g\sin(\theta(d(t))); \\ &h_2 = \tfrac{\rho\ A\ c_d}{2\ m(\xi_p)};\ h_3(r(t)) = \tfrac{r(t)}{m(\xi_p)\ r_w} \end{aligned} \tag{7}$$

These parameters depend on the gravitational acceleration, g, rolling resistance coefficient, c_r, air density, ρ, frontal vehicle area, A, air drag resistance coefficient, c_d and the vehicle mass, m respectively. The vehicle mass is determined by the powertrain design parameters $\xi_p = \{s_\tau, s_\omega, r_t\}$ for both the FGT and the CVT system. The fixed-gear ratio value for the CVT is related to the final drive ratio. The slope, θ determines the gradient resistance and is influenced by the travelled distance over time, $d(t)$. The transmission efficiency loss is modelled by a constant torque loss τ_0. The transmission efficiency becomes,

$$\eta_t(t) = \min\left(\beta(t), \beta^{-1}(t)\right) = [0,1] \in \mathbb{R}^+ \tag{8}$$

with $\beta(t) = 1 - \tau_0/\tau(t)$. Besides, the travelled distance d and the velocity v, the speed ratio r can also be seen as an additional controlled-state variable. This holds for the CVT, however, not for the FGT, as will be discussed next.

2.3 Optimal control problem: CVT, FGT

Here, the OCP for a pushbelt CVT, $\mathcal{P}_{CVT}$ and, accordingly, a FGT, $\mathcal{P}_{FGT}$, is discussed. The goal is to compare the results of both transmissions to see if using a shiftable transmission is beneficial for the energy consumption of the EV. Initially, the CVT is assumed to be lossless, i.e., $\tau_0 = 0$ Nm for simplicity. The control objective is to find the admissible optimal controls over time $\xi_c^*(t)$ consisting of the torque request u_1 and the speed ratio change command u_2, as inputs $u(t) : [0,T] \longmapsto \mathcal{U} \subseteq \mathbb{R}^m$; and, the travelled distance x_1, velocity x_2 and speed ratio x_3, as controlled-states $x(t) : [0,T] \longmapsto \mathcal{X} \subseteq \mathbb{R}^n$ that minimizes the energy J used by an EV under time and distance constraints from the beginning $t = 0$ s to the fixed end time $t = T$ s, resulting in $x_1(0) = 0$ m and $x_1(T) = D$ m. Thereby, the controls u are constraint to maximal and minimal values. Moreover, the torque constraints $(u_{1,min}, u_{1,max})$ for the machine are affected by the torque scaling factor s_τ. The velocity $x_2(t)$ and the speed ratio $x_3(t)$ are both constrained due to physical limitations of the electric machine $\omega_{max}\cdot s_\omega$. Finally, the vehicle velocity x_2 is given to be zero (standing still) and the transmission ratio x_3 to be maximal (underdrive situation) $x_{3,max}$ at $t = 0$ and at $t = T$. This results in the following OCP for the CVT, $\mathcal{P}_{CVT}$:

$$\begin{cases} \min_{\xi_c=\{x,u\}\subseteq\mathcal{X}\cap\mathcal{U}} J = \int_0^T P_m\left(x,u\right)\ \mathrm{d}t \quad \text{s.t.:} \\ \dot{x}_1(t) = x_2(t) = v(t),\ \dot{x}_3(t) = u_2(t) = \dot{r}(t) \\ \dot{x}_2(t) = h_3(x_3(t))\ u_1(t) - h_2 x_2(t)^2 - h_1(x_1(t)) - h_0 \\ \mathcal{U}: \begin{cases} u_1(t) - u_{1,max}\cdot s_\tau \le 0,\ u_{1,min}\cdot s_\tau - u_1(t) \le 0 \\ u_2(t) - u_{2,max} \le 0,\ u_{2,min} - u_2(t) \le 0 \end{cases} \\ \mathcal{X}: \begin{cases} x_2(t)\cdot x_3(t) - \omega_{max}\cdot s_\omega\cdot r_w \le 0 \\ x_3(t) - x_{3,max} \le 0,\ x_{3,min} - x_3(t) \le 0 \\ x_1(0) = 0,\ x_1(T) = D,\ x_2(0) = x_2(T) = 0 \\ x_3(0) = x_3(T) = x_{3,max} \end{cases} \end{cases} \tag{9}$$

The set $\mathcal{X}\cap\mathcal{U} \subseteq \mathbb{R}^n \cap \mathbb{R}^m$ is defined by control and state constraints, as defined above.

Necessary conditions for optimality Using the theory from PMP, the Hamiltonian, denoted as H, of the OCP is defined as,

$$H = \frac{x_3(t)}{r_w}u_1(t)x_2(t) + b_1u_1(t)^2 + b_2\frac{x_3(t)}{r_w}x_2(t) + b_3\frac{x_3(t)^3}{r_w^3}x_2(t)^3 + b_4 + \lambda_1(t)x_2(t) + \lambda_3(t)u_2(t) + \lambda_2(t)\left(\frac{x_3(t)}{m\ r_w}\ u_1(t) - h_2\ x_2(t)^2 - h_1(x_1(t)) - h_0\right) + \epsilon_1\gamma_p(x_2(t)x_3(t) - \omega_{max}s_\omega r_w) + \epsilon_2\gamma_p(x_3(t) - x_{3,max}) + \epsilon_3\gamma_p(x_{3,min} - x_3(t)) \quad (10)$$

where $\gamma_p(.)$ is described by an exterior penalty function,

$$\gamma_p(\Delta x) = \begin{cases} 0 & \text{for} \quad \Delta x \leq 0 \\ \frac{1}{2}\Delta x^2 & \text{for} \quad \Delta x > 0 \end{cases} \quad (11)$$

whereby the violation of the constraint is significantly reduced in sequential optimization steps by increasing the tuning factor ϵ_i. Now the necessary optimality conditions for the states can be defined as,

$$\dot{\lambda_1}(t) = -\frac{\partial H}{\partial x_1} = \lambda_2(t)\ \frac{\mathrm{d}h_1}{\mathrm{d}x_1} \quad (12)$$

$$\dot{\lambda_2}(t) = -\frac{\partial H}{\partial x_2} \quad (13)$$

$$= -\left(\frac{u_1(t)x_3(t)}{r_w} + b_2\frac{x_3(t)}{r_w} + 3b_3\frac{x_3(t)^3x_2(t)^2}{r_w^3}\right) + 2\lambda_2(t)h_2x_2(t) - \lambda_1(t) - x_3(t)\epsilon_1\gamma_p'(x_2(t)x_3(t) - \omega_{max}s_\omega r_w)$$

$$\dot{\lambda_3}(t) = -\frac{\partial H}{\partial x_3}$$

$$= -\left(\frac{u_1(t)x_2(t)}{r_w} + b_2\frac{x_2(t)}{r_w} + 3b_3\frac{x_3(t)^2x_2(t)^3}{r_w^3}\right) - \lambda_2(t)\frac{u_1(t)}{m\ r_w} - x_2(t)\epsilon_1\gamma_p'(x_2(t)x_3(t) - \omega_{max}s_\omega r_w) - \epsilon_2\gamma_p'(x_3(t) - x_{3,max}) + \epsilon_3\gamma_p'(x_{3,min} - x_3(t)) \quad (14)$$

where γ_p' denotes the derivative of the function γ_p to Δx of Eq. (11). The optimized control variable $u_1^*(t)$ can be calculated with,

$$\frac{\partial H}{\partial u_1} = \frac{x_2(t)\cdot x_3(t)}{r_w} + 2\cdot b_1\cdot u_1(t) + \lambda_2(t)\frac{x_3(t)}{m\cdot r_w} = 0 \quad (15)$$

which results in,

$$u_1^*(t) = -\frac{x_3(t)\cdot x_2(t)}{2\cdot b_1\cdot r_w} - \lambda_2(t)\ \frac{x_3(t)}{2\cdot b_1\cdot m\cdot r_w} \triangleq Z(t) \quad (16)$$

For notational reasons, the variable $Z(t)$ is introduced and together with the PMP method this results in the following optimal control,

$$u_1^*(t) = \begin{cases} u_{1,max}\cdot s_\tau & \text{for} \quad Z(t) > u_{1,max}\cdot s_\tau \\ Z(t) & \text{for} \quad u_{1,min}\cdot s_\tau \leq Z(t) \leq u_{1,max}\cdot s_\tau \\ u_{1,min}\cdot s_\tau & \text{for} \quad Z(t) < u_{1,min}\cdot s_\tau \end{cases} \quad (17)$$

Note that the fit coefficients b_i are also a function of the torque and speed scale parameters. The optimal control related to $u_2(t)$ results in a 'bang-bang' type of control, since minimizing the Hamiltonian H relates to minimizing $\lambda_3(t)u_2(t)$. If λ_3 is zero over a finite time, then no information on the optimal control value is available (singular control). Thereby, $\lambda_3(t)$ is often referred to as the switching function. In that case, one or more higher-order time-derivatives of the Hamiltonian are used to derive necessary conditions for optimality in the singular interval (Bell and Jacobson, 1975). Deriving these conditions for this OCP has been done, yet is quite tedious and is left out of scope here. Therefore, only the main results are presented below. If both a state constraint on the transmission ratio $x_3(t)$ and a control constraint on u_1 are active and the velocity x_2 is not constrained, then the following holds for the optimal speed ratio change: $u_2^*(t) = 0$. If, accordingly, the state constraints on the transmission ratio are not active $x_3(t) \in \langle x_{3,min}, x_{3,max}\rangle$ and both a control constraint on the torque u_1 and the path constraint on the velocity and speed ratio ($x_2(t)x_3(t) = \omega_{max}s_\omega r_w$) are active, then the optimal control u_2^* takes the following form,

$$u_2^*(t) = \dot{x}_3^*(t) = -\dot{x}_2^*(t)\cdot x_3^*(t)/x_2^*(t) \quad (18)$$

For comparison, if the path constraint of Eq. (9) is differentiated with respect to time,

$$\dot{x}_2(t)\cdot x_3(t) + x_2(t)\cdot u_2(t) = 0 \quad (19)$$

then the speed ratio change becomes,

$$u_2(t) = -\dot{x}_2(t)\cdot x_3(t)/x_2(t) = -\dot{v}(t)\cdot r(t)/v(t) \quad (20)$$

This shows that the singular control does indeed make sure that the path constraint $x_2x_3 \leq \omega_{max}s_\omega r_w$ is not violated, if the path constraint is on its boundary.

Smoothing function The control variable $u_2(t)$ takes the form of a bang-bang control and discontinuities are induced if $\lambda_2(t)$ switches sign. Therefore, a control domain smoothing technique is applied. By introducing the smoothing function from (Malisani et al., 2016), the singular control is also dealt with and higher order derivatives of the Hamiltonian do not necessarily have to be considered. In order to smoothen the function u_2 that has to be within the bounds $[u_{2,min}, u_{2,max}]$, the function $\phi(\nu(t))$ is introduced, which is given by,

$$\phi(\nu(t)) = \tanh\left(\frac{2\nu(t)}{u_{2,max} - u_{2,min}}\right) \quad (21)$$

The control input $u_2(\nu(t))$ is now introduced as,

$$u_2(\nu(t)) = \frac{u_{2,max} - u_{2,min}}{2}(\phi(\nu(t)) + 1) + u_{2,min} \quad (22)$$

which is a one to one mapping from $\mathbb{R}$ to the interior $\langle u_{2,min}, u_{2,max}\rangle$. Furthermore, a penalty function γ_u is introduced. This penalty function uses a gauge function G as argument and is given by,

$$\gamma_u \circ G_{[-1,1]}(\phi(\nu(t))) \quad (23)$$

As $G_{[-1,1]}(u) = |u|$, this can be simplified to,

$$\gamma_u(|\phi(\nu(t))|) \quad (24)$$

where $\gamma_u : [0,1\rangle \mapsto \mathbb{R}^+$. Therefore, finding γ_u is equivalent to finding $\gamma_u(\phi(\nu(t)))$ with $\gamma_u : \langle -1,1\rangle \mapsto \mathbb{R}^+$. Accordingly, the Hamiltonian can now be written as,

$$H = \frac{u_1(t)x_2(t)x_3(t)}{r_w} + b_1u_1(t)^2 + b_2\frac{x_2(t)x_3(t)}{r_w} + b_3\frac{x_3(t)^3}{r_w^3}x_2(t)^3 + + b_4 + \lambda_1(t)x_2(t) + \lambda_3(t)u_2(\nu(t)) + \lambda_2(t)\left(\frac{x_3(t)}{mr_w}u_1(t) - h_2x_2(t)^2 - h_0 - h_1(x_1(t))\right) + \epsilon_1\gamma_p(x_2(t)x_3(t) - \omega_{max}r_w) + \epsilon_2\gamma_p(x_3(t) - x_{3,max}) + \epsilon_3\gamma_p(x_{3,min} - x_3(t)) + \epsilon_4\gamma_u(\phi(\nu(t))) \quad (25)$$

Differentiating with respect to ν to find the optimal control gives,

$$\frac{\partial H}{\partial \nu} = \lambda_3(t)u_2'(\nu(t)) + \epsilon_4\gamma_u'(\phi(\nu(t)))\phi'(\nu(t)) = 0 \quad (26)$$

Where the prime denotes a derivative with respect to ν. Using Eq. (22), this can also be written as,

$$\frac{\partial H}{\partial \nu} = \frac{u_{2,max} - u_{2,min}}{2}\lambda_3(t)\phi'(\nu(t)) + \epsilon_4\gamma_u'(\phi(\nu(t)))\phi'(\nu(t)) = 0 \quad (27)$$

which simplifies to,

$$\frac{\partial H}{\partial \nu} = \lambda_3(t) + \epsilon_4\frac{2}{u_{2,max} - u_{2,min}}\gamma_u'(\phi(\nu(t))) = 0 \quad (28)$$

Following ((Malisani et al., 2016)), we define

$$\gamma_u'(\phi(\nu(t))) \triangleq \frac{u_{2,max} - u_{2,min}}{2}\sinh(\nu(t)) \quad (29)$$

As a result, the optimal control $\nu^*(t)$ is easy to find and is given by,

$$\nu^*(t) = \sinh^{-1}\Big(-\lambda_3(t)/\epsilon_4\Big) \quad (30)$$

For a small value of ϵ_4, the control $u_2(\nu^*(t))$ approaches $u_2^*(t)$.

Two-Point Boundary Value Problem The TPBVP for the OCP of $\mathcal{P}_{CVT}$ can now be given by,

$$\begin{cases} \dot{x}_1^*(t) & = x_2^*(t);\ \dot{x}_3^*(t) = u_2(\nu^*(t)) \\ \dot{x}_2^*(t) & = h_3(x_3^*(t))\cdot u_1^*(t) - h_2 x_2^*(t)^2 - h_1(x_1^*(t)) - h_0 \\ \dot{\lambda_1}^*(t) & = \lambda_2^*(t)\frac{\mathrm{d}h_1}{\mathrm{d}x_1} \\ \dot{\lambda_2}^*(t) & = -\left(\frac{x_3^*(t)u_1^*(t)}{r_w} + b_2\frac{x_3^*(t)}{r_w} + 3b_3\frac{x_3^*(t)^3x_2^*(t)^2}{r_w^3}\right) \\ & \quad +2\lambda_2^*(t)h_2x_2^*(t) - \lambda_1^*(t) \\ & \quad -x_3^*(t)\epsilon_1\gamma_p'(x_2^*(t)x_3^*(t) - \omega_{max} * r_w) \\ \dot{\lambda_3}^*(t) & = -\left(\frac{u_1^*(t)x_2^*(t)}{r_w} + b_2\frac{x_2^*(t)}{r_w} + 3b_3\frac{x_3^*(t)^2}{r_w^3}x_2^*(t)^3\right) \\ & \quad -\lambda_2^*(t)\frac{u_1^*(t)}{mr_w} - x_2^*(t)\epsilon_1\gamma_p'(x_2^*(t)x_3^*(t) - \omega_{max}r_w) \\ & \quad -\epsilon_2\gamma_p'(x_3^*(t) - x_{3,max}) + \epsilon_3\gamma_p'(x_{3,min} - x_3^*(t)) \\ x_1^*(0) & = 0,\ x_1^*(T) = D \\ x_2^*(0) & = x_2^*(T) = 0,\ x_3^*(0) = x_3^*(T) = x_{3,max} \end{cases} \quad (31)$$

The above described TPBVP for the CVT can easily be transformed into a TPBVP for a FGT by removing the control u_2 and the state x_3.

$$\mathcal{P}_{CVT} : \{u_1, u_2\} \cap \{x_1, x_2, x_3\} \longmapsto \mathcal{P}_{FGT} : \{u_1\} \cap \{x_1, x_2\}$$

Note that the singular problem is then converted into a regular OCP and no smoothing is required.

Direct method: Bocop Implementation of the above described TPBVP in Matlab for the CVT and using the `bvp4c` routine (indirect method), however, resulted in multiple numerical difficulties leading to inaccuracies, mostly related to proper guessing the initialization values. The solution is sensitive to this latter aspect. If the system specifications were changed (e.g., the bounds on the maximum gear ratio change or the torque/speed scales), it lead easily to instabilities in the whole optimization procedure. To circumvent this problem, instead of an indirect method, a direct method to transform the OCP into a nonlinear optimization problem (NLP) will be used to solve the TPBVP for both the CVT and FGT. Thereto, the open source toolbox 'Bocop' is used (Bonnans et al., 2011). This method may be less precise than the indirect approach, yet it is more robust with respect to the initialization (for the discussed design cases, yet the relative error ($< 0.6\%$) was found to be very small, e.g., FGT: 92.7 Wh with `bvp4c` and 92.3 Wh with Bocop). To solve the discretized NLP, it uses the 'Ipopt' solver, which uses a primal-dual interior point algorithm.

3. COMBINED TRANSMISSION AND CONTROL SYSTEM DESIGN OPTIMIZATION

Previously, the OCPs for the FGT and the CVT were discussed. Here, the OCPs are part of the system design, where also the electric machine size and speed ratio value r_t are being optimized. In literature, several coordination schemes for co-design can be found. For strong coupled systems, sequential or iterative design procedures may lead to suboptimal solutions or far from the global optimum, when too few iterations (due to time/budget constraints) are performed. The general co-design problem can be formulated as (Allison and Nazari, 2010),

$$\min_{\xi_p, \xi_c(t)} J(\xi_p, \xi_c(t)),\ \text{s.t. } g_{p,c}(\xi_p, \xi_c(t)) \leq 0 \quad (32)$$

where ξ_p are the plant design parameters, $\xi_c(t)$ are the (time-dependent) control variables, $J(\xi_p, \xi_c(t))$ is the system cost function and $g_p(\xi_p, \xi_c(t))$ and $g_c(\xi_p, \xi_c(t))$ are the design constraints of the plant and the control. In our design problem, an unidirectional coupling exists between the plant design constraints (via the torque, speed scale, speed ratio) and the control and state constraints. Therefore, the problem can be casted in a nested design approach,

$$\begin{array}{|ll|} \hline \textit{upper-level}: & \min\limits_{\xi_p} J^*(\xi_p) \\ & \text{s.t. } g_p(\xi_p) \leq 0 \\ \hline \textit{lower-level}: & \text{where } J^*(\xi_p) = \min\limits_{\xi_c} J(\xi_p, \xi_c(t)) \\ & \text{s.t. } g_c(\xi_p, \xi_c(t)) \leq 0 \\ \hline \end{array} \quad (33)$$

Since, in this optimization problem, including the speed scale would lead to unrealistic low speed scale values, it is kept constant at $s_\omega = 1$. For the upper-level problem

Table 1. Model parameters

Parameter (SI unit)	Value
r_w (m)	0.317
ρ (kg/m^3)	1.2
A [m2]	2.22
c_d [-]	0.31
c_r (-)	0.01
g (m/s^2)	9.81
$\theta(d)$ (-)	0
s_τ (-)	2.67
s_ω (-)	1.0
m_m (kg)	$38.1 \cdot s_\tau \cdot s_\omega$
m (kg)	$800 + m_m(s_\tau, s_\omega) + m_t(r_t)$
r_t (-): FGT	8.85
m_t (kg): FGT	$0.67 \cdot r_t^2$
m_t (kg): CVT	$0.67 \cdot r_t^2 + 50$
$x_{3,min}$ (-): CVT overdrive	1/2.15
$x_{3,max}$ (-): CVT underdrive	1/0.416
τ_0 (Nm)	{0, 5, 10}
T (s)	{25, 50, 100}
D (m)	500

of Eq. (33), a general purpose solver (GPS) is used from Matlab (`fminsearch`) and for the lower-level problem of Eq. (33), the Bocop algorithm (direct method) is used.

3.1 Co-design simulation results

In addition, to the OCP for the CVT, the maximum gear ratio change is limited by the dynamics of the CVT, resulting in additional path constraints to the original problem $\mathcal{P}_{CVT}$ in Bocop,

$$u_2(t) - u_2^+(t) \leq 0 \wedge u_2^-(t) - u_2(t) \leq 0$$

These dynamical constraints are a function of the current speed ratio or controlled state x_3. For the downshift situation (e.g., $\dot{u}_2(t) > 0$ from overdrive $x_{3,min}$ to underdrive $x_{3,max}$ and $x_{3,min} < x_{3,max}$), these dynamics are well captured with,

$$u_2^+(t) = -2.88 \cdot \Big(\ln(x_3(t)) - \ln(x_{3,max}) \Big) \cdot x_3(t) \qquad (34)$$

The gear ratio change rate for upshifting $u_2^-(t)$ is described with a second order model in (Vroemen, 2001). For simplicity, the first order model that is used for downshifting is also used for upshifting here (yet, $x_{3,max}$ is replaced with $x_{3,min}$ in Eq. (34)). Below, the influence of the transmission type (FGT vs. CVT), the CVT losses ($\tau_0 = \{0, 5, 10\}$ Nm), and the average velocity ($T = \{25, 50, 100\}$ s for constant $D = 500$ m) are investigated, respectively:

$$\left.\begin{array}{cc} \text{Type} & \{\text{FGT CVT}\} \\ \tau_0\ (\text{Nm}) & \{0 \quad 5 \quad 10\} \\ T\ (\text{s}) & \{25\ 50\ 100\} \end{array}\right\} \rightarrow \left\{\begin{array}{l} J^*(\xi_p),\ \xi_p = \{s_\tau, r_t\} \\ \xi_c^*(t) = \{u_i(t), x_i(t)\} \end{array}\right.$$

Influence on the powertrain design In Fig. 1, the minimum energy consumption $J^*(\xi_p)$ is shown as a function of the powertrain design variables ξ_p within the feasible domain $g_p(\xi_p) \leq 0$ using the parameters from Table 1. The torque scale and the transmission ratio values are both varied in discrete steps of 0.1 (-), respectively. The contour plots show the results for the lossless FGT and CVT, i.e., $\tau_0 = 0$ Nm (top-left and top-right) and for the CVT with $\tau_0 = 5$ Nm (bottom-left) and 10 Nm (bottom-right). Using the nested algorithm, the optimal design solutions (indicated with circles) for the FGT and CVT are found at $\xi^* = \{2.76, 8.85\}$ and $\xi^* = \{2.15, 5.92\}$ with an energy consumption of 92.2 Wh and 73.5 Wh, respectively. Without transmission losses, the CVT significantly improves the overall efficiency by -20.3% (-18.7 Wh) and reduces the power specification with -21.7% ($\Delta s_\tau = -0.6$). Considering the transmission losses with a $\tau_0 = 5$ Nm, resulting in an average CVT efficiency of $\overline{\eta}_t = 77\%$, the energy consumption becomes 90.9 Wh and still improves the overall efficiency by -1.4% (-1.3 Wh) and reduces the power specification with -3.9% ($\Delta s_\tau = -0.1$). Yet, if the τ_0 is set to 10 Nm ($\overline{\eta}_t = 65\%$), then the energy consumption at the optimal design of $\xi^* = \{2.87, 4.43\}$ increases by +6.7% (+6.1 Wh) compared to the lossless FGT. Notice that the small discrepancies between the minimum values from the contour plot and the found solution from the nested algorithm are caused by gridding of the search space, linear interpolation and the sensitivity of the GPS (`fminsearch`) to find a local minimum [1]. Note that the transmission masses are influenced by the gear ratio (Cf. Table 1). However, e.g., for the CVT it is found to have a negligible influence on the energy usage (appr. 200 J/kg extra energy per vehicle mass increase is needed). More results related to the J^* and ξ_p (including the values as mentioned above) can be found in Table 2. It can be observed that in comparison with a FGT (without losses) that – for lower constant torque losses ≤ 5 Nm (or average CVT power losses ≤ 1.73 kW) – the CVT reduces:

- the energy consumption J^* and depending on the losses and cycle end time, these relative values vary between {-10.3%, -1.4%} for an decreasing cycle time T or increasing average vehicle speed; and, {-20.3, -1.4%} for an increasing torque loss τ_0;
- the powertrain specification ξ_p^* and depending on the losses, there relative values for Δs_τ^* and Δr_t^* vary between {-21.7%,-3.5%} and {-50.2%, -33.3%} for a decreasing torque loss τ_0.

Table 2. System design results, $s_\omega = 1$.

Type	FGT	CVT			
T (s) — τ_0	0.0 Nm	0.0 Nm	5.0 Nm	10.0 Nm	
25	**92.2 Wh**	−18.7 Wh	−1.3 Wh	+6.1 Wh	ΔJ^*
	100 %	−20.3 %	−1.4 %	+6.7 %	
	s_τ^* **= 2.8 (-)**	−0.6	−0.1	−0.1	Δs_τ^*
	100 %	−21.7 %	−3.9 %	−3.5 %	
	r_t^* **= 8.8 (-)**	−2.9	−4.0	−4.4	Δr_t^*
	100 %	−33.3%	−45.6 %	−50.2 %	
50†	**61.2 Wh**	–	−4.7 Wh	–	ΔJ^*
	100 %	–	−7.7 %	–	
100†	**72.9 Wh**	–	−7.5 Wh	–	ΔJ^*
	100 %	–	−10.3 %	–	

† ξ_p^* constant for CVT and FGT and based on $T = 25$ s.

Moreover, the CVT seems to improve the energy efficiency in particular when the average vehicle velocity reduces. The simulation results for $T > 25$ s were based on a constant ξ_p^* design for the $T = 25$ s. The components will be oversized for lower average vehicle speeds, but are assumed, therefore, not to compromise the dynamic performance. The average efficiencies for the modelled

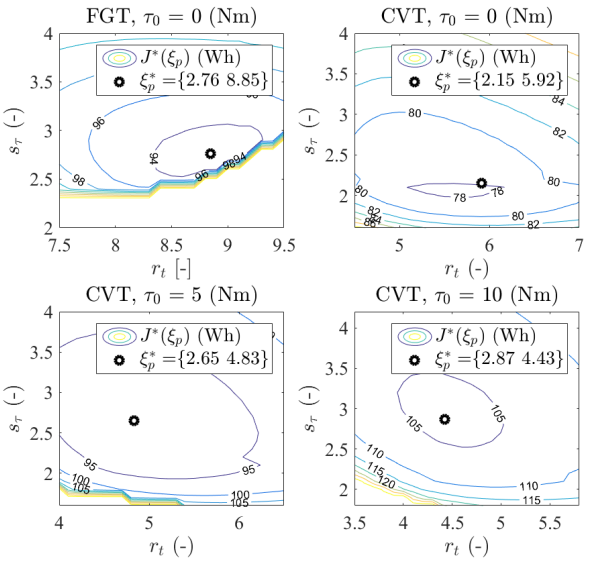

Fig. 1. Energy consumption $J^*(\xi_p)$ as a function of torque scale factor s_τ and transmission ratio r_t within the feasible domain $g_p(\xi_p) \leq 0$. Constant values: $T = 25$ s; $s_\omega = 1$ (-).

[1] Computation time, e.g., 269 s (23 iterations) and 3837 s (18 iterations) for the FGT and CVT (0 Nm, 25 s), respectively, with a CPU: Intel Core i7-3610QM.

CVTs are $\overline{\eta}_t = 77\%$ (5 Nm) and $\overline{\eta}_t = 65\%$ (10 Nm) (computed at $T = 25$ s) and are in the same order of the operation point dependent CVT (Vroemen, 2001), i.e., $\overline{\eta}_t = 72\%$ (5 Nm) and $\overline{\eta}_t = 68\%$ (10 Nm), respectively. Advanced and novel CVT systems, e.g., hydraulic-actuated (Marquenie et al., 2016) or electro-mechanical actuated CVTs (Klaassen et al., 2004) have proven to have average power losses in the order of 40 W on the WLTP or FTP72, respectively, and could, therefore, be beneficial for a (compact) EV. In future work, the influence of operation point dependent efficiency of the CVT will also be investigated.

Influence on the control design In Fig. 2, the optimal control signals for the FGT and CVT are shown. For both the FGT and CVT during the first few seconds and the last few seconds, the constraints on the input torque are active. The singular control of the gear ratio change, $u_2(t)$, is clearly visible. For the time period between 2.7 s to 5.8 s, the state constraint for the maximal vehicle velocity $x_{2,max}$ is active. This results in the singular control as defined in Eq. (20). Furthermore, the boundaries on the gear ratio x_3 are respected. Around $t = 18.5$ s, the control input torque u_1 suddenly drops as a result of the maximal vehicle velocity constraint. Since, the vehicle velocity also suddenly drops, the vehicle velocity constraint is not violated. The singular control in the gear ratio change due to the velocity constraint is again visible around $t = 19$ s.

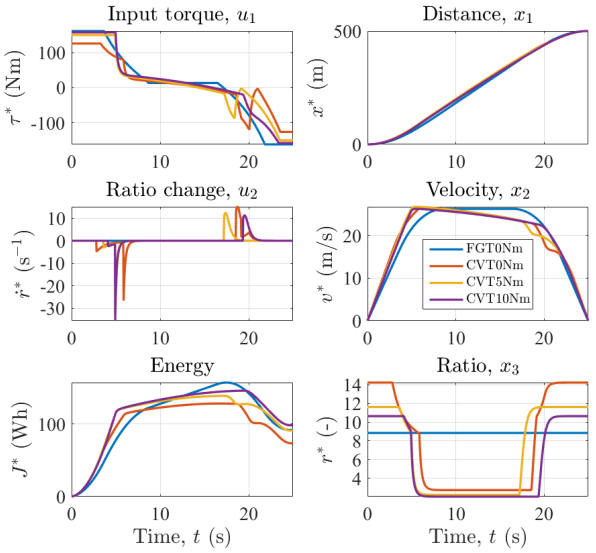

Fig. 2. Optimal control solutions ξ_c^* at the optimal transmission design ξ_p^*.

4. CONCLUSION

The OCP for the FGT and CVT has been formulated and solved using a direct method. The effects of powertrain specification on the control design and energy consumption has also been investigated. A nested approach has been adopted for finding the optimal system designs. The proposed integrated design approach clearly shows its potential in improving the overall design. A pushbelt CVT, characterized by a limited dynamic performance and relatively high actuation losses, shows it can still improve the overall efficiency and reduce the powertrain specification. In practice, the lumped (hydraulic and mechanical) torque losses of the CVT vary with the operation points and may be higher and lower than the average (constant) value assumed in this paper. However, the comparison has been done with respect to a lossless and optimized FGT. Moreover, alternative CVT actuation systems with highly-efficient components, alternative topologies and functions ('actuation on-demand') may create the required technological solutions and, accordingly, the estimated energetic and powertrain design benefits for (compact) EVs, as discussed in this paper.

REFERENCES

Allison, J. and Nazari, S. (2010). Combined plant and controller design using decomposition-base design optimization and the minimum principle. volume 1, 765–774. ASME 2010 Int. Design Engineering Technical Conferences and Computers and Information in Engineering Conference, IDETC/CIE2010. Montreal.

Bell, D. and Jacobson, D. (1975). *Singular Optimal Control Problems, Volume 117 in Mathematics in Science and Engineering*. Academic Press, New York.

Bonnans, F., Grelard, V., and Martinon, P. (2011). Bocop, the optimal control solver, open source toolbox for optimal control problems. Http://bocop.org.

Dib, W., Chasse, A., Moulin, P., Sciaretta, A., and Corde, G. (2014). Optimal energy management for an electric vehicle in eco-driving applications. *Control Engineering Practice*, 29, 299307. Saint Petersburg.

Hofman, T. and Dai, C. (2001). Energy efficiency analysis and comparison of transmission technologies for an electric vehicle. DOI: 10.1109/VPPC.2010.5729082.

Klaassen, T., Bonsen, B., van de Meerakker, K., Steinbuch, M., Veenhuizen, P., and Vroemen, B. (2004). Modelling and control of an electro-mechanically actuated pushbelt type continuously variable transmission. In *7th International Symposium on Advanced Vehicle Control (AVEC'04); Editors: J. Pauwelussen, M. Steinbuch, Arnhem, Netherlands*, 123–128.

Larminie, J. and Lowry, J. (2003). *Electric Vehicle Technology Explained*. John Wiley & Sons, Chichester.

Malisani, P., Chaplais, F., and Petit, N. (2016). An interior penalty method for optimal control problems with state and input constraints of nonlinear systems. *Optimal Control Applications and Methods*, 37(1), 3–33.

Marquenie, L., Clephas, T., and van Rooij, J. (2016). Development of an improved electro-hydraulic cvt actuator. In VDI Wissenforum 2016 (ed.), *VDI - CVT conference*.

Pontryagin, L.S., Boltyanskii, V.G., Gamkrelidze, R.V., and Mishchenko, E.F. (1962). *The Mathematical Theory of Optimal Processes*. Interscience Publishers John Wiley & Sons, Inc, New York.

Vroemen, B. (2001). *Component control for the Zero Inertia powertrain*. Phd thesis, Eindhoven University of Technology.

Wipke, K., Cuddy, M., and Burch, S. (2002). Advisor 2.1: a user-friendly advanced powertrain simulation using a combined backward/forward approach. *IEEE Transactions on Vehicular Technology*, 48(6), 1751 – 1761. DOI: 10.1109/25.806767.